



## Elaboration and characterization of chitosan/banana peel biocomposite for the removal of dyes from wastewater

Chahrazed Djilani<sup>a,d,\*</sup>, Rachida Zaghoudi<sup>b,d</sup>, Pierre Magri<sup>c</sup>, Fayçal Djazi<sup>a,d</sup>, Abdelaziz Lallam<sup>e</sup>, Bachir Bouchekima<sup>f</sup>

<sup>a</sup>Faculté de Technologie, Université du 20 Août 1955, B.P 26 Skikda 21000, Algeria, Tel. +213791665403; email: chahrazed\_dj@yahoo.fr (C. Djilani)

<sup>b</sup>Faculté des sciences, Université du 20 Août 1955, B.P 26 Skikda 21000, Algeria, Tel. +213558872108

<sup>c</sup>LCP-A2MC, EA4164, Université de Lorraine, 1, bd Arago-57078 Metz, cedex3, France, Tel. +33387315433

<sup>d</sup>Laboratoire LRPCSI, Université du 20 Août 1955, B.P 26 Skikda 21000, Algeria, Tel. +213771531297

<sup>e</sup>Laboratoire de Physique et Mécanique Textiles de l'ENSISA (LPMT), Université de Haute Alsace, 11 rue Alfred Werner, F 68093 Mulhouse CEDEX, France, Tel. +33389336900

<sup>f</sup>Laboratoire de Développement des Energies Renouvelables (LENREZA), Université Kasdi Merbah, BP 511 Ouargla 30000, Algeria, Tel. +213773725299

Received 24 September 2018; Accepted 29 January 2019

### ABSTRACT

The objective of this study is to compare the performances of chitosan/banana peel (CS/BP) biocomposite with chitosan (CS). CS, BP and CS/BP composite biomaterials were characterized by using Fourier transform infrared spectroscopy (FTIR), scanning electron microscopy (SEM) and thermal gravimetric analyses (TGA). Their specific adsorption characteristics were assessed by using a basic dye (Methylene Blue [MB]) as a model adsorbate. The influence of various experimental factors such as contact time, initial dye concentration, pH of dye solution, ionic strength and inorganic salts was investigated. The adsorption of MB from aqueous solutions was investigated using a CS/BP biocomposite and CS as adsorbents. The materials are capable of removing color from wastewater, their color removal capacity for CS is 81% and CS/banana peel biocomposite is 96% at normal pH and temperature conditions. The equilibrium times founded correspond to 150 min for CS and 100 min for CS/banana peel biocomposite. The kinetics of adsorption suggested a pseudo-second-order model fits better than pseudo-first-order model and the equilibrium isotherm fitted the Langmuir and Freundlich models. The results of this study will be useful for future scale-up using this composite biomaterial as a low-cost adsorbent for the removal of cationic dyes.

*Keywords:* Composite biomaterials; Banana peel; Chitosan; Methylene blue; Wastewater; Kinetic

### 1. Introduction

Many manufacturing industries such as textiles, paper, leather, plastics, pharmaceuticals, cosmetics, rubber, refineries, food and many other industrial fields use dyes to color their products and generate large amounts of colored effluents [1,2]. Dyes molecules are chemically stable and

difficult to be naturally biodegradable [3]. Some dyes have toxic effects to humans due to their carcinogenic, mutagenic and teratogenic effects [1,4]. Methylene blue (MB) is one of the most commonly used substances in the textile industry [5]. Although, MB is not strongly hazardous, it can cause some harmful effects, such as heartbeat increase,

\* Corresponding author.

vomiting, shock, cyanosis, jaundice, quadriplegia, and tissue necrosis in humans [6]. Several technologies have been widely employed for removal of hazardous dyes from industrial colored wastewater. These methods include chemical oxidation, microbiological degradation, coagulation-flocculation, micro and ultrafiltration, reverse osmosis, solvent extraction, evaporation, distillation, electrochemical treatment, photocatalytic degradation, adsorption, etc. [7–9]. The adsorption has been found to be superior as compared with other traditional treatment methods for wastewater treatment due to its low-cost, easy availability, simplicity of design, high efficiency, ease of operation, ability to treat dyes and eco-friendly technology to remove organic dyes from polluted water as well as low secondary pollution features [10–12]. MB has been considered as a common cationic dye model in the adsorption studies owing to its planar form [3].

Chitosan (CS) is one of the world's most plentiful and low-cost biopolymers that possess several properties which make it an ideal adsorbent for removing pollutants from wastewater [13]. CS is the result of N-deacetylation from chitin and has a chemical structure of linear chain consisting of  $\beta$ -(1,4)-linked 2-acetamino-2-deoxy- $\beta$ -D-glucopyranose with 2-amino-2-deoxy- $\beta$ -D-glucopyranose [14]. Natural polysaccharide chitosan, derivative of chitin by alkaline deacetylation, presents great interest as an organic component in the composites developed for water treatment because CS contains high units of two functional groups, hydroxyl ( $-\text{OH}$ ) and amino ( $-\text{NH}_2$ ), which are responsible for the reactivity of this polymer as an excellent natural adsorbent and give CS its powerful adsorptive capacity [15–17].

Chitin and CS are biopolymers which have excellent properties in biodegradability, biocompatibility, non-toxicity and absorption [18]. CS, because of its eco-friendly nature and macromolecular structure with different functional groups, has been found to possess many uniqueness properties that reason of recent attention in various fields, including biotechnology, water treatment, medicine, membranes, cosmetics, and the food industry [19]. The application of CS as a biopolymer adsorbent is acceptable to having the two major advantages: first, inexpensive compared with commercial adsorbents; second, strong chelating ability toward pollutants [20].

Banana is one of the most popular fruits and its cultivation is widespread in most tropical countries [21]. Banana peels have been used as food for livestock and as a biosorbent for heavy metals, dyes and for the removal of phenolic compounds [22–24].

Several studies have used CS and raw banana peel as adsorbent for removal of pollutants such as heavy metals, dyes and organic contaminants. CS has been proposed as valuable material for nanotechnology and biotechnology [19,25].

The objective of this study focuses mainly on the preparation, characterization of CS/banana peel biocomposite and the comparative evaluation of the properties of CS and CS/BP biocomposite. The effects of various analytical parameters on the adsorption of MB such as contact time, dye concentration, initial pH, ionic strength and inorganic salts were investigated. The kinetic experimental data were fitted to pseudo-first-order, pseudo-second-order and intraparticle diffusion models. The Langmuir and Freundlich isotherm equations were used to fit the equilibrium isotherm.

## 2. Materials and methods

### 2.1. Preparation of CS, BP and CS/BP biocomposite

#### 2.1.1. Preparation of banana peels

Banana peels were collected from domestic wastes and washed thoroughly with distilled water to remove the surface's adhered particles and water-soluble materials. Then it was dried with the exposure to the sun light for 4–5 d. In order to eliminate humidity and facilitate crushing, the peels were heated in an oven at 105°C. The dried banana peel was ground and sieved to obtain a particle size ranging from 150 to 250  $\mu\text{m}$  and stored in dessicator for further use.

#### 2.1.2. Synthesis of chitosan

Chitin was prepared from prawn shell waste by a chemical process involving deproteinization, demineralization and decolorization. CS was prepared from chitin by deacetylation [25].

Prawn shells were removed manually, washed under running warm tap water to remove soluble organics, adherent proteins and other impurities and solar dried for 48 h followed by oven drying at approximately 60°C for 1 h. Then, they were ground through a grinding mill.

Deproteinization is done by a solution of sodium hydroxide 2.5 N (NaOH, CAS: 1310-73-2, Mw = 40 g/mol, Biochem Chemopharma), then stirred for 6 h at a temperature of 75°C (1 g of prawn shells powder/20 ml NaOH). The samples were filtered and washed with distilled water until stabilized pH and dried in oven at 80°C for 2 h.

Calcium carbonate constitutes the main inorganic component of the shells. To remove the calcium carbonate, only dilute hydrochloric acid was used to prevent hydrolysis of chitin [26]. The deproteinized mud shrimp shells were demineralized with hydrochloric acid (HCl, CAS: 7647-01-0, Mw = 36.46 g/mol, 37%, Sigma-Aldrich). 1 g of shrimp shell powder was dissolved in HCl of 1.7 N, and then stirred with a stirrer for 6 h at a room temperature (1 g of powder/15 ml of HCl). After filtered and washed using distilled water until neutral pH and dried in an oven at 80°C for 2 h [27].

Decolorization can be done by solution of 20% hydrogen peroxide ( $\text{H}_2\text{O}_2$ , CAS: 7722-84-1, Mw = 34.02 g/mol, 30%, Biochem Chemopharma) and HCl, after filtered and washed with distilled water and dried in oven at 50°C for 24 h.

Deacetylation is the process to convert chitin to CS by removal of acetyl group. Deacetylation performed 50% NaOH at 100°C for 2 h. After filtration and washing with distilled water to remove NaOH, the obtained product is dried at 50°C for 24 h.

#### 2.1.3. Preparation of CS/BP biocomposite

1 g of CS powder was dissolved in 1 mol/L acetic acid solution (100 ml) ( $\text{C}_2\text{H}_4\text{O}_2$ , CAS: 64-19-7, Mw = 60.05 g/mol, 99%, Sigma-Aldrich), and mixed with 1 g of Banana peel and stirred for 1 h at 20°C. Then CS /banana peel biocomposite was washed using distilled water and dried in an oven at 60°C for 24 h. After drying, it was ground and sieved [28].

## 2.2. Characterization methods

The morphology, structure and properties of CS, BP and CS/BP biocomposite were determined by Fourier transform infrared spectroscopy (FTIR), scanning electron microscopy (SEM) and thermal gravimetric analyses (TGA).

FTIR was used to detect the functional groups present at the surface of the adsorbent. The spectra were recorded in the frequency range of 650–4,000  $\text{cm}^{-1}$  using an FTIR spectrophotometer (FTIR-8400S SHIMADZU).

The microstructure of the adsorbent was observed using a scanning electron microscope (HITACHI S-2360 N).

Thermogravimetric analysis (TGA/DTG) allows for the continuous recording of the mass changes of a sample with linearly increasing temperature. The apparatus used was a 2050 TGA V5.4A from TA Instruments. The thermal evolution of CS, BP and CS/BP biocomposite were followed by TGA from room temperature up to 1,000°C of CS, 600°C of BP and 1,000°C of CS/BP biocomposite. TGA/DTG curves were recorded with a 10°C/min heating rate under nitrogen atmosphere and an approximate mass of 20 mg.

## 2.3. Batch adsorption experiments

MB is usually discharged in high levels in industrial wastewater, specially textiles, papers and cosmetics industries. The complex structure of MB dye makes it very stable and difficult to degrade leading to many environmental problems. In this reason, MB was selected as a model dye because of its ability to be strongly adsorbed onto solid materials.

Adsorption studies of Methylene blue (MB; molecular formula is  $\text{C}_{16}\text{H}_{18}\text{ClN}_3\text{S}$ ; C.I.No.52015; Mw = 319.85; Biochem Chemopharma) was performed using CS and CS/BP biocomposite as the adsorbents.

The batch experiments were performed using a set of 250 ml stoppered flasks (Erlenmeyer flasks) containing a known quantity of adsorbents (0.10 g) and a pre-defined volume (100 ml in each flask) of dye solution at a fixed initial concentration (10 mg/L) with a constant pH of the solution. The flasks were then placed in a shaker at 250 rpm and a temperature of 25°C. The samples were examined at specific time intervals, and the solutions were filtered at equilibrium using 0.45  $\mu\text{m}$  filter paper to determine the equilibrium concentrations.

The initial and equilibrium concentrations were measured with a Shimadzu UV-1700 spectrophotometer at wavelengths of 665 for MB.

The amount of dye adsorbed onto the adsorbent at equilibrium,  $q_e$  (mg/g), was calculated by the following expression:

$$q_e = \frac{(C_i - C_e) \cdot V}{W} \quad (1)$$

where  $C_i$  and  $C_e$  are the initial and equilibrium concentrations in mg/L, respectively,  $W$  is the mass of the CS and CS/BP biocomposite expressed in g and  $V$  is the volume of the solution in L.

The dye removal efficiency ( $R$ ) was calculated by the following equation:

$$R(\%) = \frac{C_i - C_e}{C_i} \times 100 \quad (2)$$

The amount of adsorption at time  $t$ ,  $q_t$  (mg/g) was calculated by:

$$q_t = \frac{(C_i - C_t) \cdot V}{W} \quad (3)$$

where  $C_t$  (mg/L) is the liquid concentration of dye at any time and  $C_i$  (mg/L) is the initial concentration of the dye in solution,  $W$  is the mass of CS and CS/BP biocomposite expressed in g and  $V$  is the volume of the solution in L.

In order to evaluate the effect of parameters influencing the adsorption of MB, we studied the effect of a series of factors likely to intervene in the process of this phenomenon.

## 2.4. Kinetic models

In the present study, the adsorption kinetics of MB on CS and CS/BP biocomposite was modelled using three common models: the pseudo-first-order [29], pseudo-second-order [30], intraparticle diffusion [31] models.

Several equations can be used to express the equilibrium elimination of an adsorption process. In this investigation, the Langmuir and Freundlich isotherm functions were used to evaluate the elimination of the dyes from aqueous solution [32,33].

## 3. Results and discussion

### 3.1. Characterization of CS, BP and CS/BP biocomposite

#### 3.1.1. IR spectroscopy

FTIR were used to examine functional group distributions in the CS, BP and CS/BP biocomposite, Fig. 1(a) shows the FTIR of CS, BP and CS/BP biocomposite before adsorption and Figs. 1(b)–(c) shows the FTIR of CS and CS/BP biocomposite after adsorption.

The main characteristic absorption peaks of CS at 3,435, 2,879, 1,619, 1,553, 1,375, 1,041 and 880  $\text{cm}^{-1}$  were attributed respectively, to O–H and N–H symmetric stretching vibration, to C–H stretching vibration of the aliphatic, to N–H bending vibrations of primary amine group of CS, to N–H bending of secondary amine, to C–N stretching vibration, to C–O stretching vibration, and  $\gamma(\text{C-H})$  in the aromatic ring [26,34,35].

FTIR spectra of banana peel displayed a number of peaks pertaining to different functional groups. The broad absorption peak at 3,285  $\text{cm}^{-1}$  corresponds to the O–H stretching vibration of alcohols, phenols and carboxylic acids as in pectin, cellulose, hemicellulose and lignin [36]. Thus, showing the presence of «free» hydroxyl groups on the adsorbent surface [23]. Bands appearing at 2,918, 1,735, 1,600, 1,374, 1,028 and 868  $\text{cm}^{-1}$  in Fig. 1 were assigned to C–H stretching vibrations (hemicelluloses and cellulose bonds), C=O stretching of carbonyl group (hemicellulose band), COO<sup>-</sup> anion stretching, OH bending, C–O stretching of ester or ether and N–H deformation of amines, respectively [37,38].

The spectrum of the CS/BP biocomposite (Fig. 1(a)) shows the combination of characteristic absorptions specific for both components (CS and BP). The broad absorption peak at 3,285  $\text{cm}^{-1}$  corresponds to combination of characteristic

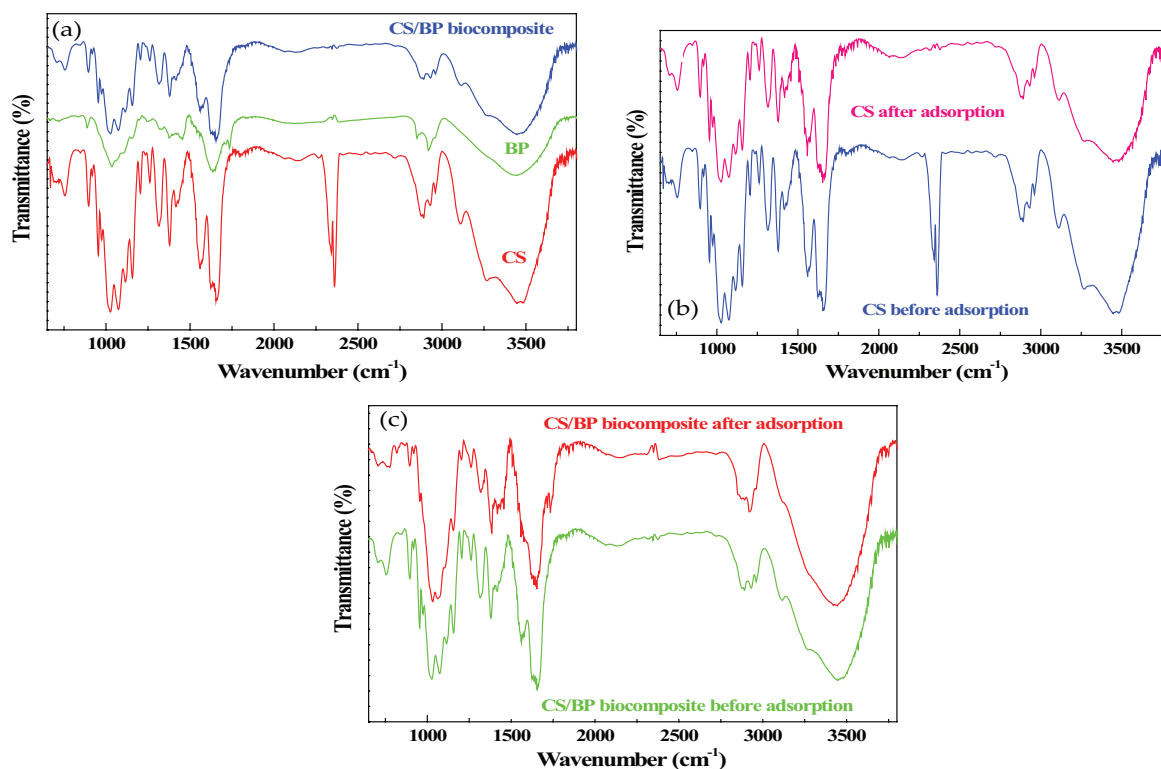


Fig. 1. FTIR of CS before and after adsorption, CS/Banana peel biocomposite before and after adsorption and Banana peel.

peaks of O–H and  $\text{NH}_2$ . Bands appearing at 2,918, 1,735, 1,600, 1,553, 1,375 and 1,028  $\text{cm}^{-1}$  in Fig.1 were assigned to C–H stretching vibrations of the aliphatic (hemicelluloses and cellulose bonds), C=O stretching of carbonyl group (hemicellulose band), to N–H bending vibrations of primary amine group of CS, to N–H bending of secondary amine, C–O stretching of ester or ether, respectively [34,36].

The spectrum of CS after adsorption (Fig. 1(b)) showed similar characteristics as the CS before adsorption except for slight changes. Some peaks shifted after adsorption whereas other peaks disappeared after adsorption. The FTIR spectrum of CS/BP biocomposite (Fig. 1(c)) indicates that the peaks are slightly shifted from their position and the intensity gets altered. Because of the surface loading of adsorbent by dye molecules, the absorption peaks were transferred to higher frequency region [39]. This was a clear indication that adsorption of MB onto CS and CS/BP biocomposite take place and new bonds were formed between CS-MB cation and CS/BP biocomposite-MB cation.

Two possible mechanisms of adsorption of MB may be considered (Fig. 2): (a) electrostatic interaction between the groups of adsorbents (CS and CS/BP biocomposite) and the MB dye, and (b) the chemical reaction between the adsorbate and the adsorbents [40].

### 3.1.2. Surface morphology

Scanning electron microscopy (SEM) has been a primary tool for characterizing the surface morphology and fundamental physical properties of the adsorbent. SEM images of BP and of CS and CS/BP biocomposite adsorbents were taken before and after dye adsorption on MB are presented in Fig. 3.

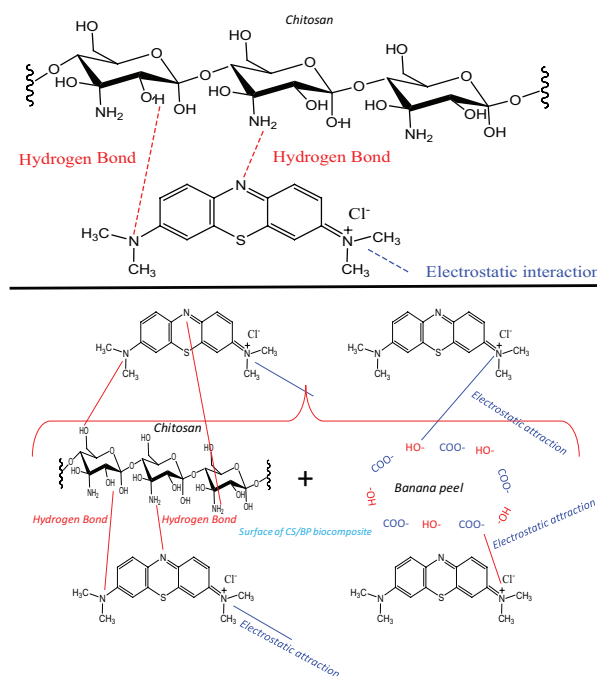


Fig. 2. Adsorption mechanism of MB dye onto CS and CS/BP biocomposite.

From (Figs. 3), it is clear, there is a good possibility for dyes to be trapped and adsorbed into these pores.

CS sample exhibited rough, highly corrugated and thick surface (Fig. 3). The banana peel is a heterogeneous material and an irregular surface morphology. CS/BP biocomposite

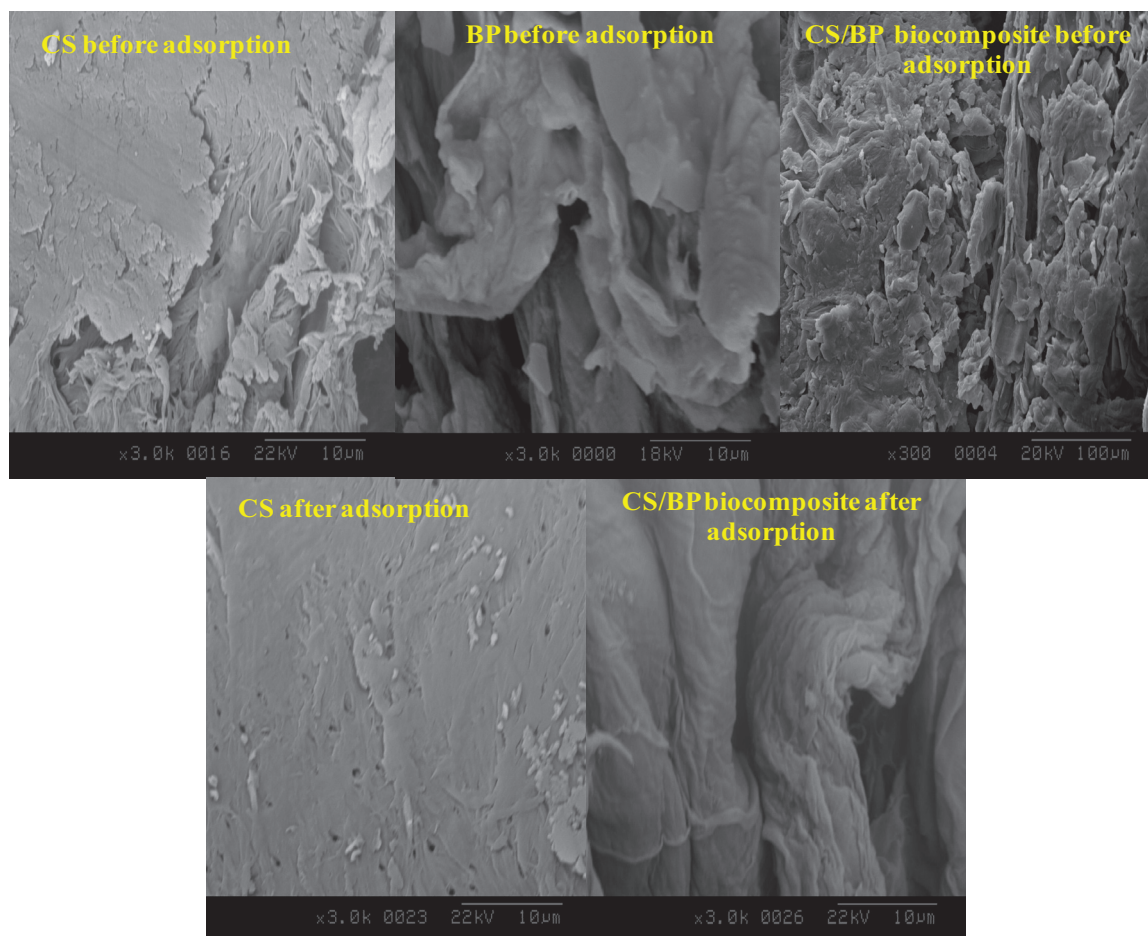


Fig. 3. SEM images of CS, Banana peel and Chitosan/Banana peel biocomposite before adsorption, Chitosan and Chitosan/Banana peel biocomposite.

images (Fig. 3) show an irregular surface and some cracks and channels, which can be associated to internal pores with smaller diameters. However, the surface morphology of CS/BP biocomposite is different from that of CS and natural BP. The surface morphology of bioadsorbent became much smoother after the adsorption of MB, and pores and caves are filled by MB dye.

### 3.1.3. Thermal gravimetric analyses

Fig. 4 shows the thermogravimetric (TGA) and derivative thermogravimetric (DTG) curves of CS, banana peel and the biocomposite obtained from CS and banana peel. In case of CS, the weight loss around 42°C is attributed to the loss of superficial moisture from the CS. A major weight loss at 378°C is due to the degradation of CS molecule [41].

The TGA record of the powdered banana peels (Fig. 4) shows four stages of the decomposition reaction. The first weight loss around 86°C is due to the physisorbed water departure. The continuous loss of mass between 150°C and 400°C corresponding to three major stage (173°C, 285°C and 355°C), is due to the decomposition of hemicellulose depolymerized, cellulose and lignin [42].

The TGA and DTG curves of biocomposite indicate three mass loss stages: moisture evaporation up to about 44°C,

main decomposition of biocomposite matrix between 200°C and 400°C, and continuous slight decomposition thereafter (about 887°C) corresponding to the carbonization of CS/BP biocomposite.

## 3.2. Effects of various parameters influencing the adsorption

### 3.2.1. Effect of contact time

Contact time is inevitably a fundamental parameter in all transfer phenomena such as adsorption. The effect of contact time on the adsorption of MB by CS and CS/BP biocomposite are shown in Fig. 5. The amount of the absorbed MB onto CS and CS/BP biocomposite initially, increase with time and at some point of time, it reaches a constant value beyond which no more is removed from solution. The amount of MB adsorbed at the equilibrium time reflects the maximum adsorption capacity of the adsorbent under those operating conditions. The adsorption curves are single, smooth, and continuous leading to saturation and indicate the possible monolayer coverage on the surface of adsorbents by the MB dye molecules [43].

The percentage removal of CS was 81% at 150 min and CS/BP biocomposite was 96% at 100 min, this is due to the saturation of the active sites which cannot let further adsorption

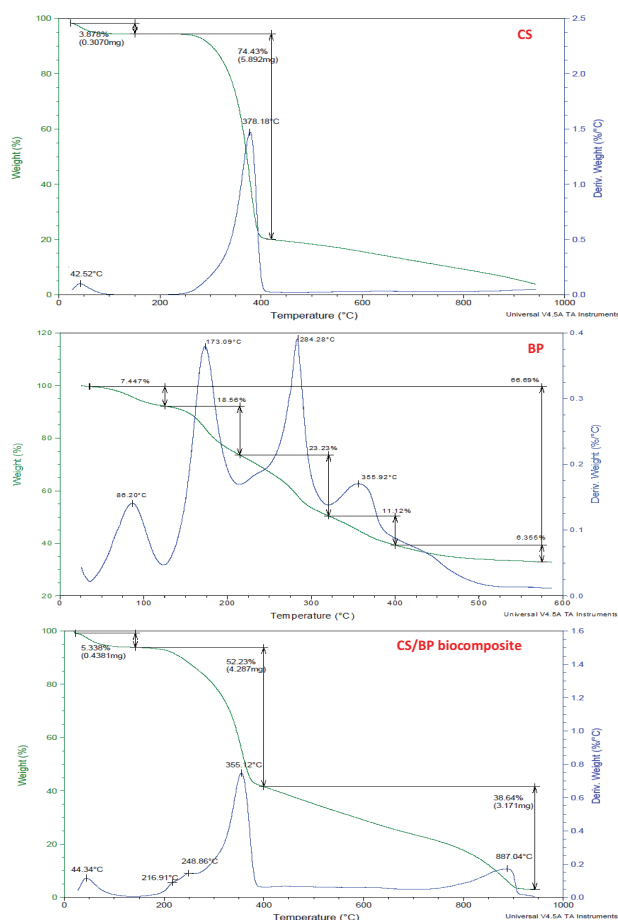


Fig. 4. ATG of CS, Banana peel and Chitosan/Banana peel biocomposite.

to take place. It is evident that the bioadsorbent are efficient in absorbing equilibrium gradually. It is obviously the rate of adsorption and adsorption capacity of MB onto CS/BP biocomposite is more than CS.

### 3.2.2. Effect of initial dye concentration

The dye concentration also plays an important role in the adsorption capacity of adsorbents. Six different concentrations 5, 10, 20, 30, 40 and 50 mg/L were selected to investigate the effect of the initial dye concentration on the adsorption of MB on CS and CS/BP biocomposite. The other process parameters were kept constant, including the solution pH, 0.10 g of adsorbent, a temperature of 25°C and an agitation speed of 250 rpm.

As expected the removal capacity of all the adsorbents increased with increasing initial concentration (figure not shown). The removal of MB increased from 56% to 80% for CS and from 89% to 95% for CS/BP biocomposite when initial concentration of MB was increased from 5 to 50 mg/L, respectively.

It can be stated that a higher initial MB concentration results in the increase in driving force between the aqueous solution and solid phases, thus increasing the uptake. This leads to enhanced the number of collisions between the dye

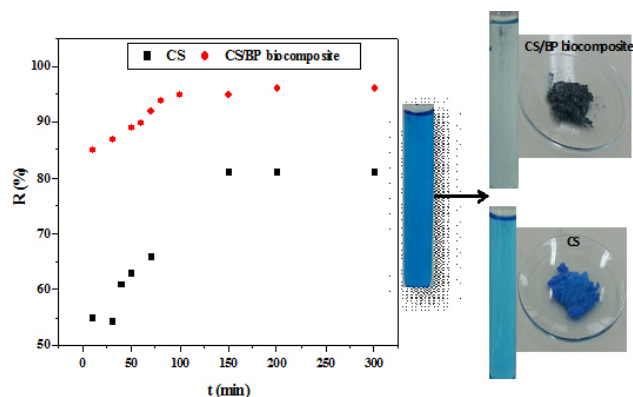


Fig. 5. Effect of contact time on MB % dye removal onto CS and CS/BP biocomposite ( $[C]_{MB}$ : 10 mg/L,  $T$ : 25°C,  $m_{CS/CS/BP}$  biocomposite: 0.10 g, agitation speed: 250 rpm and  $pH_{MB}$  4.85).

molecules and the adsorbent (CS and CS/BP biocomposite) and decreased resistance to the uptake of dye molecules from colored solution improving the amount of adsorbed dye [44].

### 3.2.3. Effect of pH

The pH value of the dye solution is an important factor for the determination the adsorption of solutes. The solution pH can affect the surface charge of the adsorbent and the dissociation of functional groups on the active sites of the adsorbent as well as the structure of the dye molecule [17].

Solution pH was studied by varying the initial pH of solution from 2 to 10. The adsorbents dosage, rotation speed, temperature and initial dye concentration were fixed at 0.10 g, 250 rpm, 25°C and 10 mg/L.

The removal percentage of MB on CS/BP biocomposite increased significantly with an increase in the solution pH, primarily due to the protonation of the MB in the acidic medium and the presence of excess  $H^+$  ions competing with dye cations for adsorption sites [45].

The reverse was observed for MB on CS (figure not shown), the adsorption of MB onto CS is most important in acid medium. There is a significant decrease in the amount adsorbed of MB in range pH of 6–10. The maximum removal of MB onto CS (77%) at pH 4.

The maximum MB dye removal when the pH of the solution was increased, the positive charges on the solution interface decreased and the adsorbent surface appeared negatively charged.

### 3.2.4. Effect of ionic strength

The wastewater containing dye has commonly higher salt concentration, and ionic strength effect is of some importance in dye adsorption onto adsorbents. The ionic strength of the solution is one of the factors that control both electrostatic and non-electrostatic interactions between the adsorbate and the adsorbent surface [46].

The effect of salt concentration (NaCl) on the removal of MB was studied at different NaCl concentrations of 0.2, 0.4 and 1 mol/L with a fixed adsorbent dosage of 0.10 g, a temperature of 25°C and an agitation speed of 250 rpm as shown in Fig 6.

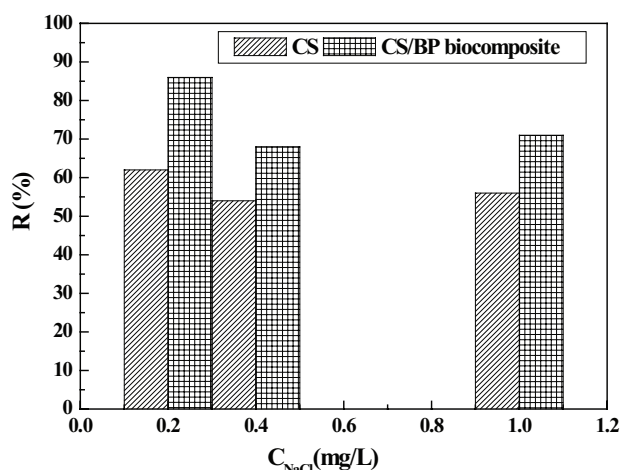


Fig. 6. Effect of ionic strength on MB % dye removal onto CS and CS/BP biocomposite ( $[C]_{MB}$ : 10 mg/L,  $T$ : 25°C,  $m_{CS/CS/BP}$  biocomposite: 0.10 g, agitation speed: 250 rpm and  $pH_{MB}$  4.85).

The percentage removal of MB decreased from 62% to 57% and from 86% to 71% for CS and CS/BP biocomposite, respectively, as the ionic strength concentrations increased from 0.2 to 1 mol/L.

This could be attributed to the competitive effect between dye cations and  $Na^+$  ions for the available adsorption sites; similar observation has been reported [47,48].

As the ionic strength increased, the activity of MB and the active sites for adsorption decreased, therefore, the adsorption amount of MB decreased [49].

### 3.2.5. Effect of inorganic salts

The occurrence of various types of salts is rather common in colored textile effluents. The salts could change the ionic nature, hydrophobicity, size, and solubility of the dye and their presence leads to high ionic strength, which may significantly affect the performance of dye adsorption process [6].

The effect of several inorganic salts ( $NaCl$ ,  $Na_2SO_4$  and  $Na_2HPO_4$ ) on MB adsorption by CS and CS/BP biocomposite was studied. 0.2 M of each of  $NaCl$ ,  $Na_2SO_4$ ,  $Na_2HPO_4$  were prepared and 25 ml of each were mixed with 10 mg/L of MB containing 0.10 g of CS and CS/BP biocomposite under shaker. The MB removal percentages were measured in the absence and presence of  $NaCl$ ,  $Na_2SO_4$  and  $Na_2HPO_4$ , as shown in Fig. 7.

The effect was referred to competition between the salts anions  $Cl^-$ ,  $SO_4^{2-}$  and  $HPO_4^{2-}$  and the MB for the unoccupied sites on the CS and CS/BP biocomposite.

In the absence of  $NaCl$ ,  $Na_2SO_4$  and  $Na_2HPO_4$ , MB dye removal percentage at equilibrium can reach 81% and 96% onto CS and CS/BP biocomposite, respectively. By comparison, MB dye removal percentage at equilibrium decreased to 62% (CS) and 85% (CS/BP biocomposite) in the presence  $NaCl$ , to 45% (CS) and 78% (CS/BP biocomposite) in the presence  $Na_2SO_4$ , to 48% (CS) and 79% (CS/BP biocomposite) in the presence  $Na_2HPO_4$ .

The highest removal percentage of MB by CS/BP biocomposite is in the presence of  $NaCl$ ,  $Na_2SO_4$  and  $Na_2HPO_4$ ,

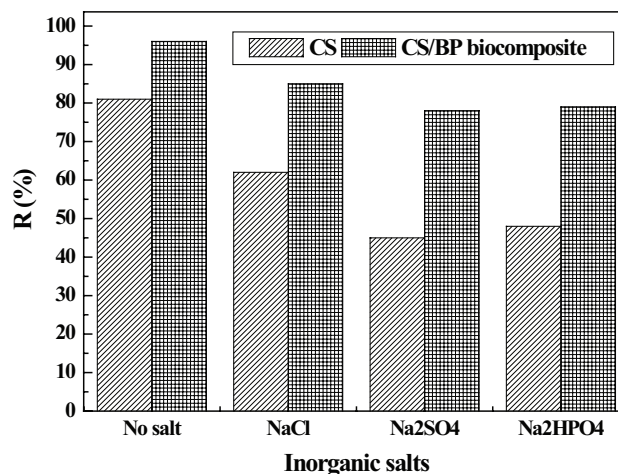


Fig. 7. Effect of Inorganic salts on MB % dye removal onto CS and CS/BP biocomposite ( $[C]_{MB}$ : 10 mg/L,  $T$ : 25°C,  $m_{CS/CS/BP}$  biocomposite: 0.10 g, agitation speed: 250 rpm and  $pH_{MB}$  4.85).

the competition due to the high negative charges of  $Cl^-$ ,  $SO_4^{2-}$ ,  $HPO_4^{2-}$  and MB onto sites of CS/BP biocomposite.

### 3.3. Adsorption kinetics

Adsorption kinetic describes the controlling mechanism of adsorption processes which in turn governs the mass transfer and equilibrium time. The experimental data of MB adsorption onto CS and CS/BP biocomposite at different time intervals were examined using pseudo-first-order, pseudo-second-order and intraparticle diffusion kinetic models.

The MB adsorption onto CS and CS/BP biocomposite was fitted by three kinetic models, and values of  $k_1$ ,  $k_2$ ,  $k_{int}$  and  $q_{calc}$  as well as correlation coefficients are listed in Table 1. The correlation coefficients ( $R^2$ ) of MB for the pseudo-second-order model onto CS and CS/BP biocomposite were 0.9924 and 0.9997, respectively. On the other hand, the correlation coefficients of MB for the pseudo-first-order kinetics model onto CS and CS/BP biocomposite were 0.9304 and 0.9782, respectively.

Based on Table 1, the  $R^2$  value obtained from the intraparticle diffusion kinetic model were 0.8814 and 0.9676 onto CS and CS/BP biocomposite, respectively. The results show that the correlation coefficient for the intraparticle diffusion kinetic model was lower than the second-order and first-order kinetic models.

The kinetic linearized model studies showed that the pseudo-second-order kinetic model with high correlation coefficient described the system much better than the first-order kinetic model and the intraparticle diffusion of MB onto CS and CS/BP biocomposite, the adsorption of MB onto CS and CS/BP biocomposite fit this model.

The applicability of the pseudo-second-order kinetic model suggested that the adsorption MB onto CS and CS/BP biocomposite is based on chemical reaction (chemisorptions), which involved valency forces through sharing or exchange of electrons between the adsorbent and adsorbate [50].

3.4. Adsorption isotherms

The Langmuir and Freundlich adsorption isotherm constants for MB adsorption are presented in Table 2. A comparison of the  $R^2$  values obtained from the adsorption models clearly indicates that the Langmuir and Freundlich models provides the best fit for the adsorption of MB on CS and CS/BP biocomposite.

The applicability of the Langmuir isotherm suggests the monolayer coverage of the dye on the homogeneous surface of CS and CS/BP biocomposite. The maximum adsorption

capacity of MB by CS and CS/BP biocomposite were 64.72, 35.57 mg/g, respectively. The adsorption capacity of CS/BP biocomposite for MB was higher than the value of CS. Furthermore, the  $K_L$  value of CS/BP biocomposite was higher than that of CS, indicating that CS/ BP biocomposite had the highest adsorption energy.

The Freundlich model is applied to describe a heterogeneous system characterized by a heterogeneity factor of  $1/n$ . This model describes reversible adsorption. The values of correlation coefficients and other parameters obtained from CS and CS/BP biocomposite are given in Table 2. The  $n$  values were all more than 1 ( $n > 1$ ) indicating that the Freundlich type adsorption is favorable.

A comparative evaluation of the adsorbents capacities of various types of adsorbents for the adsorption of MB is listed in Table 3.

Table 1

Pseudo-first order, pseudo-second order and intraparticle diffusion kinetic model parameters for the adsorption of MB onto CS and CS/BP biocomposite

	CS	CS/BP biocomposite
Pseudo-first-order model	$\log(q_e - q_t) = \log q_e - \frac{k_1}{2,303} \times t$	
$q_{e,calc}$ (mg/g)	3.108	24.087
$k_1$ (min <sup>-1</sup> )	0.0099	0.0094
$R^2$	0.9304	0.9782
Pseudo-second-order model	$\frac{t}{q_t} = \frac{1}{k_2 q_e^2} + \frac{1}{q_e} t$	
$q_{e,calc}$ (mg/g)	0.5581	3.0779
$k_2$ (g/mg. min)	28.015	1.0248
$R^2$	0.9924	0.9997
Intraparticle diffusion	$q_t = k_{int} t^{1/2}$	
$k_{int}$ (mg/g.min <sup>1/2</sup> )	0.4925	1.3818
$R^2$	0.8814	0.9676

$k_1$  and  $k_2$ : rate constants for the pseudo-first, pseudo-second-order adsorption and  $k_{int}$ : intraparticle diffusion constant.

Table 2

Langmuir and Freundlich isotherm constants and correlation coefficients for adsorption of MB on CS and CS/BP biocomposite

Models	Parameters	CS	CS/BP biocomposite
Langmuir isotherm	$\frac{1}{q_e} = \frac{1}{q_{max}} + \frac{1}{K_L \cdot q_{max}} \times \frac{1}{C_e}$		
	$q_{max}$ (mg/g)	35.57	64.72
	$K_L$ (L/mg)	0.0155	0.0220
	$R^2$	0.9934	0.9986
Freundlich isotherm	$\ln q_e = \ln K_F + \frac{1}{n} \ln C_e$		
	$K_F$ ((mg/g)(L/mg) <sup>1/n</sup> )	2.0608	3.0767
	$n$	1.0279	1.0851
	$R^2$	0.9952	0.9937

Table 3

Comparison of maximum adsorption capacity of dyes by some adsorbents

Adsorbents	Dyes	$q_{max}$ (mg/g)	References
H <sub>2</sub> SO <sub>4</sub> crosslinked magnetic chitosan nanocomposite beads	Methylene blue	20.408	[5]
Activated lignin-chitosan extrudates	Methylene blue	36.25	[15]
Carboxymethyl cellulose/k-carrageenan/activated montmorillonite composite beads	Methylene blue	10.75	[3]
Carbon/ montmorillonite (CMt) nanocomposites	Methylene blue	138.10	[51]
Cellulose/graphene oxide composite aerogel	Methylene blue	78.493	[11]
Banana peel	Methylene blue	20.8	[52]
Biocomposites with peanut waste biomass (Native, Chitosan aniline, Chitosan pyrrole, Strach)	Crystal violet	33.23	[53]
		54.91	
		150.16	
		10.25	
Brown macroalga	Methylene blue	95.45	[54]
Chitosan	Methylene blue	35.57	This study
CS/BP biocomposite	Methylene blue	64.72	This study



#### 4. Conclusion

The present study indicates that CS/banana peel biocomposite have been successfully prepared from CS and banana peel. The larger adsorption capacity of CS/BP biocomposite may be the reason for larger area for synthesis of biocomposite. Scanning electron microscopy micrographs of CS/BP biocomposite revealed that the surface was highly porous in nature. The interaction between CS and banana peel was confirmed by FTIR spectroscopy and SEM imaging. The difference in surface morphology of adsorbents before and after adsorption and the shifting of peaks in FTIR spectrum confirmed the MB dye adsorption onto CS and CS/BP biocomposite. The maximum adsorption of MB was obtained as 64.72 and 35.57 mg/g for CS/BP biocomposite and CS, respectively. The kinetics of adsorption suggested a pseudo-second-order model fits better than pseudo-first-order model for MB. The equilibrium adsorption process was best fitted by the Langmuir and Freundlich models. The experimental results showed that the biocomposite could potentially be used in the removal of the cationic dyes in aqueous solutions and industrial wastewater treatments.

#### Acknowledgements

The authors would like to thank the Laboratory LCP-A2MC of Université de Lorraine-France and especially Dr. Pierre MAGRI for his assistance in TGA/DDSC analyses.

#### References

- [1] B. Xu, H. Zheng, Y. Wang, Y. An, K. Luo, C. Zhao, W. Xiang, Poly (2-acrylamido-2-methylpropane sulfonic acid) grafted magnetic chitosan microspheres: preparation, characterization and dye adsorption, *Int. J. Biol. Macromol.*, 112 (2018) 648–655.
- [2] X. Wang, C. Jiang, B. Hou, Y. Wang, C. Hao, J. Wu, Carbon composite lignin-based adsorbents for the adsorption of dyes, *Chemosphere*, 206 (2018) 587–596.
- [3] C. Liu, A.M. Omer, X-kun Ouyang, Adsorptive removal of cationic methylene blue dye using carboxymethyl cellulose/k-carrageenan/activated montmorillonite composite beads: isotherm and kinetic studies, *Int. J. Biol. Macromol.*, 106 (2018) 823–833.
- [4] A. Nasrullah, A.H. Bhat, A. Naeem, M. Hasnain Isa, M. Danish, High surface area mesoporous activated carbon-alginate beads for efficient removal of methylene blue, *Int. J. Biol. Macromol.*, 107 (2018) 1792–1799.
- [5] Rahmi, Ishmaturrehmi, I. Mustafa, Methylene blue removal from water using H<sub>2</sub>SO<sub>4</sub> crosslinked magnetic chitosan nanocomposite beads, *Microchem. J.*, 144 (2019) 397–402.
- [6] A.K. Kushwaha, N. Gupta, M.C. Chattopadhyaya, Removal of cationic methylene blue and malachite green dyes from aqueous solution by waste materials of *Daucus carota*, *J. Saudi. Chem. Soc.*, 18 (2014) 200–207.
- [7] N.A. Abdelwahab, E.M.H. Morsy, Synthesis and characterization of methyl pyrazolone functionalized magnetic chitosan composite for visible light photocatalytic degradation of methylene blue, *Int. J. Biol. Macromol.*, 108 (2018) 1035–1044.
- [8] Y.L. Cao, Z.H. Pan, Q.X. Shi, J.Y. Yu, Modification of chitin with high adsorption capacity for methylene blue removal, *Int. J. Biol. Macromol.*, 114 (2018) 392–399.
- [9] T.N. Vieira de Souza, S.M. Leão de Carvalho, M.G.A. Vieira, M.G. Carlos da Silva, D.S.B. Brasil, Adsorption of basic dyes onto activated carbon: experimental and theoretical investigation of chemical reactivity of basic dyes using DFT-based descriptors, *Appl. Surf. Sci.*, 448 (2018) 662–670.
- [10] M. Açıkıldız, A. Gürses, S. Karaca, Preparation and characterization of activated carbon from plant wastes with chemical activation, *Microporous Mesoporous Mater.*, 198 (2014) 45–49.
- [11] F. Ren, Z. Li, W.Z. Tan, X.H. Liu, Z.F. Sun, P.G. Ren, D.X. Yan, Facile preparation of 3D regenerated cellulose/graphene oxide composite aerogel with high-efficiency adsorption towards methylene blue, *J. Colloid. Interface. Sci.*, 532 (2018) 58–67.
- [12] L. Meng, X. Xu, B. Bai, M. Ma, S. Li, N. Hu, H. Wang, Y. Suo, Surface carboxyl-activated polyester (PET) fibers decorated with glucose carbon microspheres and their enhanced selective adsorption for dyes, *J. Phys. Chem. Solids.*, 123 (2018) 378–388.
- [13] M. Vakili, M. Rafatullah, B. Salamatinia, A.Z. Abdullah, M.H. Ibrahim, K.B. Tan, Z. Gholami, P. Amouzgar, Application of chitosan and its derivatives as adsorbents for dye removal from water and wastewater, *Carbohydr. Polym.*, 113 (2014) 115–130.
- [14] R. Salehi, M. Arami, N.M. Mahmoodi, H. Bahrami, S. Khorramfar, Novel biocompatible composite (Chitosan–zinc oxide nanoparticle): preparation, characterization and dye adsorption properties, *Colloids. Surf. B. Biointerfaces.*, 80 (2010) 86–93.
- [15] A.B. Albadarin, M.N. Collins, M. Naushad, S. Shirazian, G. Walker, C. Mangwandi, Activated lignin–chitosan extruded blends for efficient adsorption of methylene blue, *Chem. Eng. J.*, 307 (2017) 264–272.
- [16] S.M. Dehaghi, B. Rahmanifar, A.M. Moradi, P.A. Azar, Removal of permethrin pesticide from water by chitosan–zinc oxide nanoparticles composite as an adsorbent, *J. Saudi. Chem. Soc.*, 18 (2014) 348–355.
- [17] S. Çınar, Ü.H. Kaynar, T. Aydemir, S.Ç. Kaynar, M. Ayvacklı, An efficient removal of RB5 from aqueous solution by adsorption onto nano-ZnO/Chitosan composite beads, *Int. J. Biol. Macromol.*, 96 (2017) 459–465.
- [18] V. Nair, A. Panigrahy, R. Vinu, Development of novel chitosan–lignin composites for adsorption of dyes and metal ions from wastewater, *Chem. Eng. J.*, 254 (2014) 491–502.
- [19] Y. Jiang, J.L. Gong, G.M. Zeng, X.M. Ou, Y.N. Chang, C.H. Deng, J. Zhang, H.Y. Liu, S.Y. Huang, Magnetic chitosan–graphene oxide composite for anti-microbial and dye removal applications, *Int. J. Biol. Macromol.*, 82 (2016) 702–710.
- [20] M.S. Kiakhani, M. Arami, K. Gharanjig, Preparation of chitosan–ethyl acrylate as a biopolymer adsorbent for basic dyes removal from colored solutions, *J. Environ. Chem. Eng.*, 1 (2013) 406–415.
- [21] H. Tibolla, F.M. Pelissari, F.C. Menegalli, Cellulose nanofibers produced from banana peel by chemical and enzymatic treatment, *LWT-Food Sci. Technol.*, 59 (2014) 1311–1318.
- [22] A. Ali, K. Saeed, F. Mabood, Removal of chromium (VI) from aqueous medium using chemically modified banana peels as efficient low-cost adsorbent, *Alexandria. Eng. J.*, 55 (2016) 2933–2942.
- [23] V.S. Munagapati, V. Yarramuthi, Y. Kim, K.M. Lee, D.S. Kim, Removal of anionic dyes (Reactive Black 5 and Congo Red) from aqueous solutions using Banana Peel Powder as an adsorbent, *Ecotoxicol. Environ. Saf.*, 148 (2018) 601–607.
- [24] A. Ali, Removal of Mn (II) from water using chemically modified banana peels as efficient adsorbent, *Environ. Nanotechnol. Monit. Manage.*, 7 (2017) 57–63.
- [25] A.J. Al-Manhel, A.R.S. Al-Hilphy, A.K. Niamah, Extraction of chitosan, characterisation and its use for water purification, *J. Saudi. Soc. Agric. Sci.*, 17 (2018) 186–190.
- [26] S.Kumari, P.K. Rath, Extraction and characterization of chitin and chitosan from Labeo rohita fish, *Procedia Mater. Sci.*, 6 (2014) 482–489.
- [27] M.S. Benhabiles, R. Salah, H. Lounici, N. Drouiche, M.F.A. Goosen, N.Mameri, Antibacterial activity of chitin, chitosan and its oligomers prepared from shrimp shell waste, *Food. Hydrocolloids.*, 29 (2012) 48–56.
- [28] Q. Liu, B. Yang, L. Zhang, R. Huang, Adsorption of an anionic dye by cross-linked chitosan/bentonite composite, *Int. J. Biol. Macromol.*, 72 (2015) 1129–1135.
- [29] C. Escudero, C. Gabaldón, P. Marzal, I. Villaescusa, Effect of EDTA on divalent metal adsorption onto grape stalk and exhausted coffee wastes, *J. Hazard. Mater.*, 152 (2008) 476–485.
- [30] N. Azouaou, Z. Sadaoui, A. Djaafri, H. Mokaddem, Adsorption of cadmium from aqueous solution onto untreated coffee

- grounds: equilibrium, kinetics and thermodynamics, *J. Hazard. Mater.*, 184 (2010) 126–134.
- [31] S. Liang, X. Guo, N. Feng, Q. Tian, Isotherms, kinetics and thermodynamic studies of adsorption of  $\text{Cu}^{2+}$  from aqueous solutions by  $\text{Mg}^{2+}/\text{K}^{+}$  type orange peel adsorbents, *J. Hazard. Mater.*, 174 (2010) 756–762.
- [32] A. Aziz, E.H. Elandaloussi, B. Belhafaoui, M.S. Ouali, L. Charles De Ménorval, Efficiency of succinylated-olive stone biosorbent on the removal of cadmium ions from aqueous solutions, *Colloids. Surf., B.*, 73 (2009) 192–198.
- [33] H. Lalruaitluanga, K. Jayaram, M.N.V. Prasad, K.K. Kumar, Lead(II) adsorption from aqueous solutions by raw and activated charcoals of *Melocanna baccifera* Roxburgh (bamboo)—A comparative study, *J. Hazard. Mater.*, 175 (2010) 311–318.
- [34] S. Hydari, H. Sharififard, M. Nabavinia, M. reza Parvizi, A comparative investigation on removal performances of commercial activated carbon, chitosan biosorbent and chitosan/activated carbon composite for cadmium, *Chem. Eng. J.*, 193–194 (2012) 276–282.
- [35] M. Abbasian, M. Jaymand, P. Niroomand, A.F. Habibi, S.G. Karaj-Abad, Grafting of aniline derivatives onto chitosan and their applications for removal of reactive dyes from industrial effluents, *Int. J. Biol. Macromol.*, 95 (2017) 393–403.
- [36] D. Pathania, S. Sharma, P. Singh, Removal of methylene blue by adsorption onto activated carbon developed from *Ficus carica* bast, *Arab. J. Chem.*, 10 (2017) S1445–S1451.
- [37] A.M. Aljeboree, A.N. Alshirifi, A.F. Alkaim, Kinetics and equilibrium study for the adsorption of textile dyes on coconut shell activated carbon, *Arab. J. Chem.*, 10 (2017) S3381–S3393.
- [38] H. Pereira de Carvalho, J. Huang, M. Zhao, G. Liu, L. Dong, X. Liu, Improvement of Methylene Blue removal by electrocoagulation/banana peel adsorption coupling in a batch system, *Alexandria. Eng. J.*, 54 (2015) 777–786.
- [39] Sidra Shoukat, Haq Nawaz Bhatti, Munawar Iqbal, Saima Noreen, Mango stone biocomposite preparation and application for crystal violet adsorption: a mechanistic study, *Microporous Mesoporous Mater.*, 239 (2017) 180–189.
- [40] Li Wang, A. Wang, Adsorption properties of congo red from aqueous solution onto N,O-carboxymethyl-chitosan, *Bioresour. Technol.*, 99 (2008) 1403–1408.
- [41] A. Nithya, H.L. Jeeva Kumari, K. Rokesh, K. Ruckmani, K. Jothivenkatachalam, A versatile effect of chitosan-silver nanocomposite for surface plasmonic photocatalytic and antibacterial activity, *J. Photochem. Photobiol., B*, 153 (2015) 412–422.
- [42] P.D. Pathak, S.A. Mandavgane, Preparation and characterization of raw and carbon from banana peel by microwave activation: application in citric acid adsorption, *J. Environ. Chem. Eng.*, 3 (2015) 2435–2447.
- [43] A.S. Sartape, A.M. Mandhare, V.V. Jadhav, P.D. Raut, M.A. Anuse, S.S. Kolekar, Removal of malachite green dye from aqueous solution with adsorption technique using *Limonia acidissima* (wood apple) shell as low cost adsorbent, *Arab. J. Chem.*, 10 (2017) S3229–S3238.
- [44] K. Amela, M.A. Hassen, D. Kerroum, Isotherm and kinetics study of biosorption of cationic dye onto banana peel, *Energy Procedia.*, 19 (2012) 286–295.
- [45] C. Djilani, R. Zaghdoudi, F.Djazi, B. Bouchekima, A. Lallam, A. Modarressi, M. Rogalski, Adsorption of dyes on activated carbon prepared from apricot stones and commercial activated carbon, *J. Taiwan Inst. Chem. Eng.*, 53 (2015) 112–121.
- [46] K. Ellass, A. Laachach, A. Alaoui, M. Azzi, Removal of methyl violet from aqueous solution using a stevensite-rich clay from Morocco, *Appl. Clay Sci.* 54 (2011) 90–96.
- [47] N. Gupta, A.K. Kushwaha, M.C. Chattopadhyaya, Application of potato (*Solanum tuberosum*) plant wastes for the removal of methylene blue and malachite green dye from aqueous solution, *Arabian. J. Chem.*, 9 (2016) S707–S716.
- [48] R. Han, W. Zou, W. Yu, S. Cheng, Y. Wang, J. Shi, Biosorption of methylene blue from aqueous solution by fallen phoenix tree's leaves, *J. Hazard. Mater.*, 141 (2007) 156–162.
- [49] L.B.L. Lim, N. Priyantha, D.T.B. Tennakoon, H.I. Chieng, M. Suklueng, Breadnut peel as a highly effective low-cost biosorbent for methylene blue: equilibrium, thermodynamic and kinetic studies, *Arab. J. Chem.*, 10 (2017) S3216–S3228.
- [50] K.Y. Foo, B.H. Hameed, Microwave-assisted preparation and adsorption performance of activated carbon from biodiesel industry solid residue: influence of operational parameters, *Bioresour. Technol.*, 103 (2012) 398–404.
- [51] D.S. Tong, C.W. Wu, M.O. Adebajo, G.C. Jin, W.H. Yu, S. Fu Ji, C.H. Zhou, Adsorption of methylene blue from aqueous solution onto porous cellulose derived carbon/montmorillonite nanocomposites, *Appl. Clay Sci.*, 161 (2018) 256–264.
- [52] G. Annadurai, R.-Shin Juang, D.-Jong Lee, Use of cellulose-based wastes for adsorption of dyes from aqueous solutions, *J. Hazard. Mater.*, 92 (2002) 263–274.
- [53] N. Tahir, H.N. Bhatti, M. Iqbal, S. Noreen, Biopolymers composites with peanut hull waste biomass and application for Crystal Violet adsorption, *Int. J. Biol. Macromol.*, 94 (2017) 210–220.
- [54] E. Daneshvar, A. Vazirzadeh, A. Niazi, M. Kousha, M. Naushad, A. Bhatnagar, Desorption of Methylene blue dye from brown macroalga: effects of operating parameters, isotherm study and kinetic modeling, *J. Clean. Prod.*, 152 (2017) 443–453.